Human Molecular Genetics, 2010, Vol. 19, No. 20 **3906–3918**
doi:10.1093/hmg/ddq330
Advance Access published on August 6, 2010

Arrhythmia and cardiac defects are a feature of spinal muscular atrophy model mice

Christopher R. Heier[1,2], Rosalba Satta[1,2], Cathleen Lutz[3] and Christine J. DiDonato[1,2,*]

[1]Human Molecular Genetics Program, Children's Memorial Research Center, 2300 Children's Plaza, PO Box 211, Chicago, IL 60614, USA, [2]Department of Pediatrics, Feinberg School of Medicine, Northwestern University, Chicago, IL 60611, USA and [3]The Jackson Laboratory, 600 Main Street, Bar Harbor, ME 04609, USA

Received June 3, 2010; Revised July 13, 2010; Accepted July 30, 2010

Proximal spinal muscular atrophy (SMA) is the leading genetic cause of infant mortality. Traditionally, SMA has been described as a motor neuron disease; however, there is a growing body of evidence that arrhythmia and/or cardiomyopathy may present in SMA patients at an increased frequency. Here, we ask whether SMA model mice possess such phenotypes. We find SMA mice suffer from severe bradyarrhythmia characterized by progressive heart block and impaired ventricular depolarization. Echocardiography further confirms functional cardiac deficits in SMA mice. Additional investigations show evidence of both sympathetic innervation defects and dilated cardiomyopathy at late stages of disease. Based upon these data, we propose a model in which decreased sympathetic innervation causes autonomic imbalance. Such imbalance would be characterized by a relative increase in the level of vagal tone controlling heart rate, which is consistent with bradyarrhythmia and progressive heart block. Finally, treatment with the histone deacetylase inhibitor trichostatin A, a drug known to benefit phenotypes of SMA model mice, produces prolonged maturation of the SMA heartbeat and an increase in cardiac size. Treated mice maintain measures of motor function throughout extended survival though they ultimately reach death endpoints in association with a progression of bradyarrhythmia. These data represent the novel identification of cardiac arrhythmia as an early and progressive feature of murine SMA while providing several new, quantitative indices of mouse health. Together with clinical cases that report similar symptoms, this reveals a new area of investigation that will be important to address as we move SMA therapeutics towards clinical success.

INTRODUCTION

Spinal muscular atrophy (SMA) is the leading monogenic cause of infant mortality (1). It is caused by insufficient dosage of the *survival motor neuron* (*SMN*) genes. Patients are homozygous for *SMN1* deletion or loss of function mutations and possess varying copy numbers of the nearly identical but alternatively spliced *SMN2* gene (2–4). The low levels of SMN protein produced from *SMN2* result in a disease pathology that is characterized by motor neuron loss and skeletal muscle atrophy. However, a growing number of SMA case studies suggest cardiac and autonomic complications may either be associated with SMA or be uncovered as patient survival is extended by improved medical intervention.

Recently, a comprehensive survey of 63 severe SMA (Type I) patients attending one pediatric clinic found that 24% presented with severe symptomatic bradycardia, with four of these patients dying as bradycardia progressed to cardiac standstill (5). In addition to these severe patients, instances of heart block progressing to complete atrioventricular (AV) block have been observed in adults with mild SMA (Type III) (6–8). Arrhythmias such as these can develop from either autonomic nervous system (ANS) defects or from cardiomyopathies. ANS symptoms such as hyperhidrosis and poor circulation have long been casually observed in SMA patients. Case studies confirm that such effects can manifest in tachyarrhythmia, altered RR interval variation, decreased sympathetic skin response and affected vasodilation in severe to intermediate SMA (9–11). Cardiomyopathies have also been observed to co-occur with SMA, in both Type I and Type III patients (6,8,10,12–17). In addressing this issue, a recent study focusing on severe SMA by *Schoneborn et al*. (18) found that three out of four random patients possessing a single copy of *SMN2* had

*To whom correspondence should be addressed. Tel: +1 7737556352; Fax: +1 7737556345; Email: c-didonato@northwestern.edu

congenital septal defects, a complication that statistically should only co-occur with SMA in 1 out of 50 million individuals.

With a growing body of evidence that arrhythmia and/or cardiomyopathy may be present in SMA patients with increased frequency, we ask here whether or not SMA model mice show such phenotypes. We find that SMA mice suffer from severe bradyarrhythmia. A natural history of SMA heart rhythms reveals that SMA mice present with bradycardia as early as 2 days of age, before quantifiable onset of neuromuscular symptoms. Their bradyarrhythmia is characterized by progressive heart block and reduced ventricular depolarization efficiency. Further investigations show evidence of both ANS defects and cardiomyopathy at the late stages of disease. Drug-based rescue of SMA survival demonstrates the utility of the electrocardiogram (ECG) as a quantitative, non-invasive biomarker, with the progression of bradycardia further predictive of death events in mice that exhibit extended survival without progression of neuromuscular phenotypes. Together, these data represent the novel identification of cardiac arrhythmia as an early and progressive feature of murine SMA. With a growing number of case studies and findings in comparable diseases, it is essential that we determine the full extent of cardiac involvement in patients as we move forward in developing therapeutics capable of extending survival.

RESULTS

We utilized the *SMNΔ7* SMA mouse model (JAX line 5025) developed by Le *et al*. (19) for these studies. In our laboratory (20) and in agreement with previous studies (19,21), this model exhibited a phenotype apparent by postnatal day (PND) 5 with an average survival of approximately 2 weeks. Debilitating neuromuscular symptoms were overtly visible by PND8, at which point ambulation was severely affected and mice were grossly undersized. Around PND10, SMA mice began to lose weight and exhibit a decreased level of consciousness (LOC). All ECG values were obtained from resting heart rates recorded using a non-invasive method described previously (22), with a sample size of ten mice unless otherwise noted.

SMA mice exhibit bradyarrhythmia

To determine whether SMA mice show functional cardiac abnormalities, we examined ECGs recorded from affected mutants and unaffected carrier mice. Readings at PND8, when mutant mice show overt SMA symptoms, revealed that bradyarrhythmia was present in SMA mice relative to unaffected heterozygous littermates (Fig. 1). To further examine the electrophysiological nature and developmental time course of cardiac arrhythmia in SMA mice, we characterized the natural history of ECG waveform parameters throughout the development of SMA mice and their control littermates.

ECG waveforms established in previous works are equivalent in males and females during neonatal time points (22,23). To provide further baseline data in our control genotypes of mice, we recorded ECGs from ages PND2 to PND14 in unaffected mice that were either wild-type at the endogenous *Smn* locus ($Smn^{+/+}$) or heterozygous at the endogenous locus ($Smn^{+/-}$). All mice were homozygous for the two transgenes present in this model ($SMN2^{+/+}$;$SMN\Delta7^{+/+}$). No difference in heart rate between genotypes was detected at any time point assayed (Fig. 2), nor was any difference observed in PR interval duration, QRS interval duration or in measures of heart rate variability (data not shown). Comparison with the previous data obtained from wild-type FVB/N mice showed that all values and time points were consistent with established ECG values (22). Together, this demonstrated that there is no effect of transgene insertion or *Smn* heterozygosity on heart rate or other ECG waveforms.

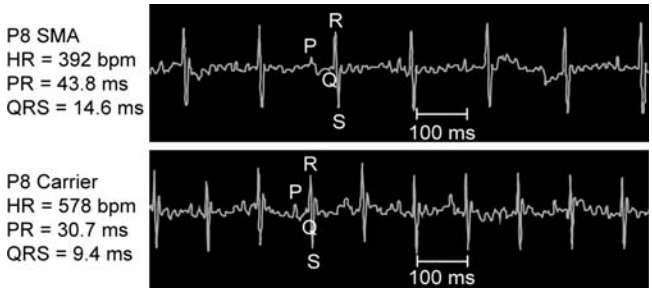

Figure 1. Conscious SMA mice exhibit bradycardia. Initial survey of several SMA mice revealed a reduction in heart rate in comparison to control littermates. Tracings here come from representative ECGs obtained in conscious SMA (top) and unaffected heterozygous (bottom) mice. Some tremor of the isoelectric line is present in all readings due to the mice being conscious and unrestrained. Individual waveforms are denoted by P, Q, R or S. Scale bar = 100 ms.

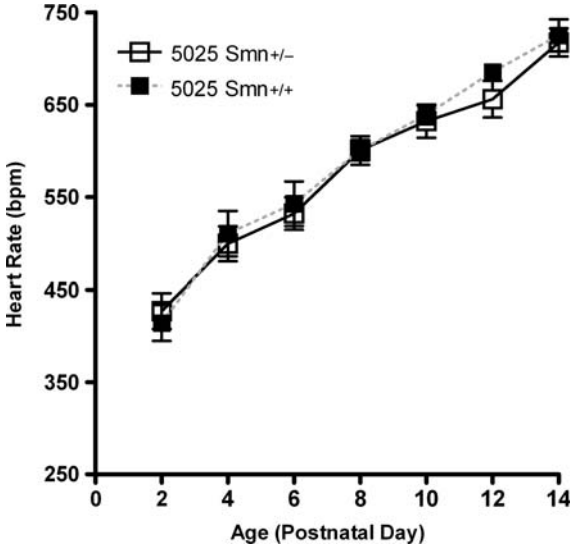

Figure 2. Transgenic background has no effect on ECG. ECGs were recorded every 2 days from unaffected 5025 mice that were either homozygous wild-type ($Smn^{+/+}$) or heterozygous carriers of a knockout allele ($Smn^{+/-}$) at the *Smn* locus. All data were obtained from conscious, unrestrained mice, with heart rate presented here as mean ± SEM. No differences were present between genotypes at any time point in this or other ECG parameters (n = 10 mice per data point).

Bradyarrhythmia with progressive heart block and impaired conduction

Heart rates were reduced in SMA mice at all time points examined (Fig. 3A). At PND2, the earliest age we could

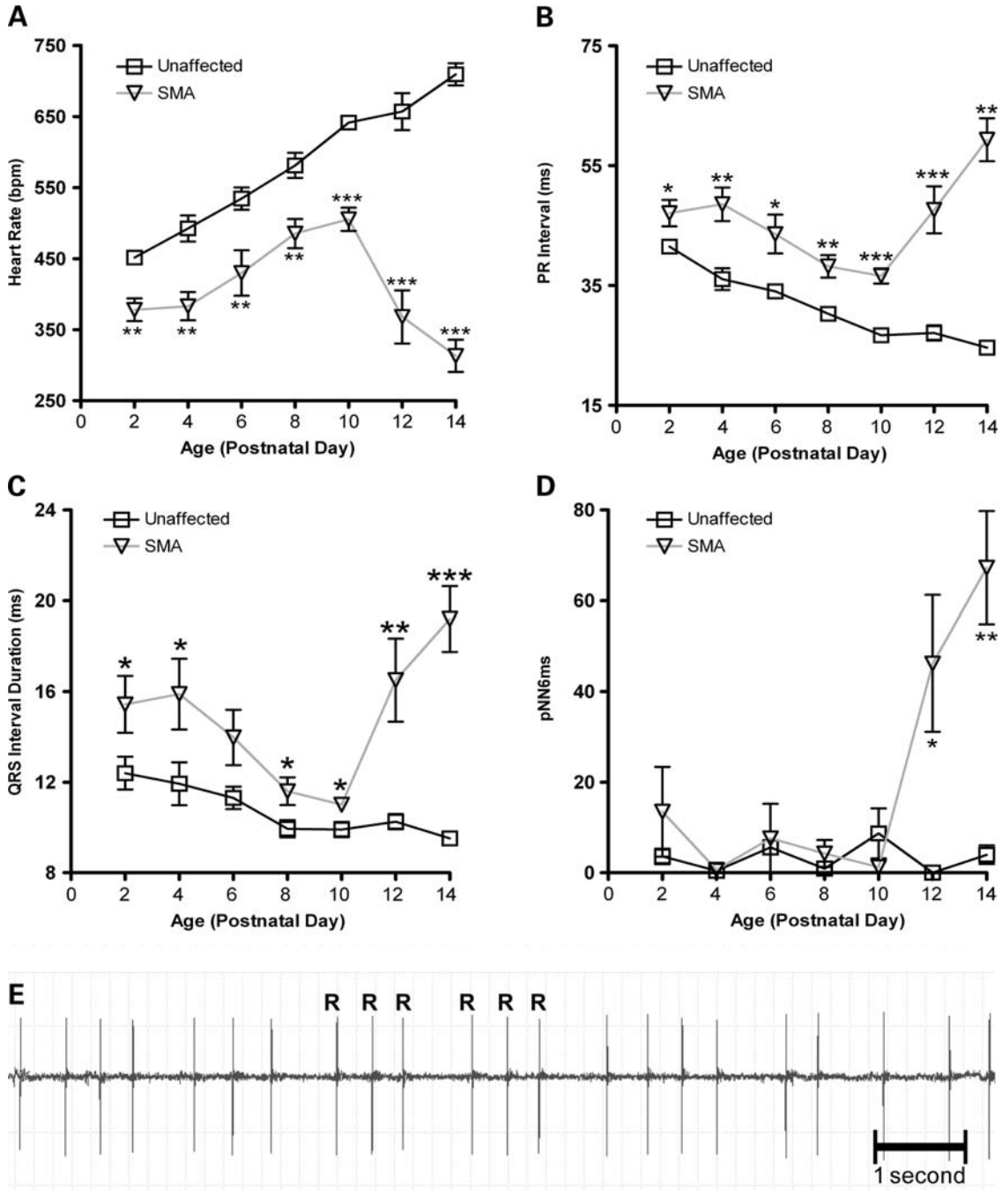

Figure 3. Life history of arrhythmia in SMA mice. Resting ECGs recorded for SMA and unaffected littermates every 2 days reveal significant physiological differences in waveforms. All mice were conscious and unrestrained. (**A**) Heart rate, (**B**) PR interval, (**C**) QRS interval and (**D**) pNN6ms values are expressed as mean ± SEM. (*$P < 0.05$, **$P < 0.005$, ***$P < 5E^{-6}$, $n = 10$ mice per data point). (**E**) Representative ECG from a PND14 mouse that displayed progressive heart block manifesting in skipped beats.

reliably assay, SMA mice had an average heart rate of 378 ± 50 b.p.m., whereas unaffected littermates had a heart rate of 451 ± 22 b.p.m. ($n = 10$ per genotype, $P \leq 0.0005$). From PND4 to PND8, SMA heart rates increased at a steady rate of approximately 25 b.p.m. each day, consistent with littermate controls as well as previous studies characterizing the development of neonatal heart rhythms (22). Throughout this time, SMA mice exhibited heart rates that were approximately 100 b.p.m. lower than unaffected mice. At PND10, the heart rate of SMA mice became further reduced compared with control mice (505 ± 51 versus 642 ± 24 b.p.m., respectively). This deficit progressed at PND12 and PND14 where there was a large drop from previous time points in the heart rate of SMA mice. This resulted in heart rates in SMA mice that were approximately half those in unaffected mice as they

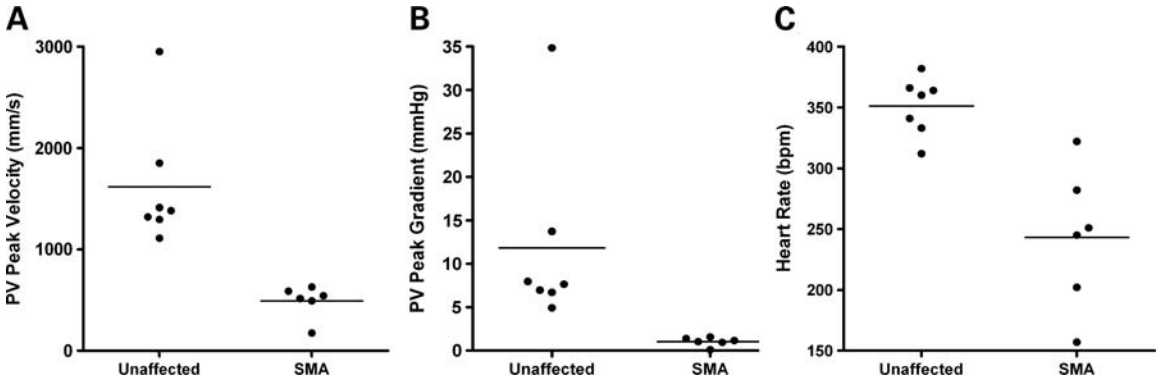

Figure 4. Echocardiography deficits in SMA mice. Echocardiography was performed on sedated PND6 mice. SMA mice had depressed values in (**A**) PV peak velocity ($P < 0.005$) and (**B**) PV peak gradient ($P < 0.05$). (**C**) Heart rate was decreased in sedated mice when compared with conscious mice. Consistent with data from conscious mice, SMA mice showed reduced heart rates compared with control littermates ($P < 0.005$; $n = 6–7$ mice per genotype).

approached death endpoints (368 ± 119 versus 657 ± 83 b.p.m.; $P < 5E^{-11}$). Together, these results elucidate two points. First, a significant bradyarrhythmia phenotype is present in SMA mice as early as PND2. Second, the end stage of life in SMA mice is characterized by severe bradyarrhythmia progressing to cardiac standstill.

The most common cause of bradyarrhythmia is heart block, detected through the elongation of PR interval duration. In SMA mice, PR interval was significantly elongated at every time point ECGs were recorded (Fig. 3B). As with heart rate, PR interval showed two phases during the growth of SMA mice. At PND4, SMA mice possessed a first-degree heart block characterized by elongated PR interval durations compared with unaffected littermates (48.6 ± 8.8 versus 36.1 ± 5.7 ms, $P \leq 0.001$); this was maintained as PR interval development paralleled that of unaffected mice until PND10. After this age, there was a sharp increase in the PR interval and breakdown of the cardiac rhythm as mice exhibited progressive heart block as they neared the end stage of survival.

We detected a significant elongation of the time of ventricular depolarization for SMA mice through an increase in QRS interval duration, beginning by PND4 (Fig. 3C). At this point, SMA mice possessed a QRS interval lasting 15.9 ± 4.9 ms, compared with 11.9 ± 3.0 ms for unaffected littermates ($P \leq 0.05$). Ventricular depolarization times were precisely maintained in unaffected mice. SMA mice exhibited larger variations in this parameter as they matured until around PND10, at which point there was a sharp increase as mice began to approach death endpoints.

We found low values of heart rate variability in unaffected neonate mice, as previously observed in neonatal stages of humans and multiple mammalian species (24–27). However, as SMA mice neared the end stage of disease, they displayed a sharp spike in measures of heart rate variability (Fig. 3D). This manifested in ECGs as heart rhythms that were erratic and/or contained skipped beats (Fig. 3E). Ultimately, SMA mice displayed adjacent RR intervals that were highly inconsistent, resulting in average pNN6 values of ~50–60% for PND12 and PND14 mice. Thus, roughly half of the consecutive heart beats in end stage SMA mice differed in duration by an amount significantly exceeding the threshold set for a regular rhythm.

Functional deficits detected by echocardiography

Echocardiography was performed on PND6 mice to gain further insight into the level of cardiac function in SMA mice. Deficiencies in blood flow out of the right ventricle were detected at the pulmonary valve in SMA mice. Peak velocity was significantly decreased in all SMA mice relative to all littermate controls (489.7 ± 162.2 versus 1617.09 ± 630.2 mm/s; $P < 0.005$), as was peak gradient (1.1 ± 0.5 versus 11.8 ± 10.5 mmHg; $P < 0.05$) (Fig. 4A and B). In both groups, heart rates measured while performing echocardiography were lower than previous measurements due to the mice being sedated. Consistent with earlier findings, however, heart rates were significantly lower in SMA mice than in controls (243 ± 58 versus 351 ± 24 b.p.m.; $P < 0.005$) (Fig. 4C). Thus, the SMA heart shows significant reductions in both pumping efficiency and blood flow from the right ventricle to the lungs. Together, these data establish that gross deficits in cardiac function are present in neonate SMA mice.

Examination of SMA heart morphology and sympathetic innervation

We examined heart to body size ratios to determine whether gross defects in heart morphology were present. Defects such as cardiac hypertrophy or hypotrophy could affect cardiac function and result in hemodynamic insufficiency during periods of normally rapid development in growing SMA neonates. After peaking at PND10, SMA mice typically lost weight each day before dying around 13 days of age. Accordingly, we sacrificed mice at PND10 and PND13 to examine the heart at these two points. General observation of heart morphology and histological sections (data not shown) were entirely consistent with vehicle groups presented later, with SMA mouse hearts appearing smaller and flaccid while lacking defined shape with gross attenuation of walls. Here, SMA mice sacrificed at PND13 lost an average of 21 ± 5% of their body weight, whereas unaffected genotypes gained an average of 26 ± 5% (Fig. 5A). We found at PND10 that SMA mice displayed a heart to body weight ratio comparable to that of unaffected littermates. At PND13, that ratio was

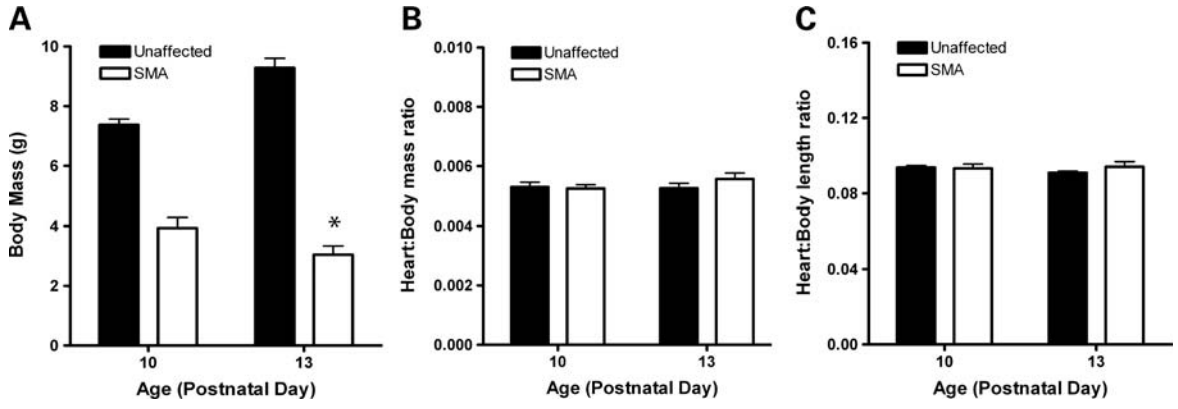

Figure 5. Loss of cardiac mass in end stage of life. (**A**) Body mass decreased 21 ± 5% in SMA mice from PND10 to PND13, whereas that of unaffected littermates increased by 26 ± 5% (*$P < 0.05$, $n = 7$ mice per genotype). (**B**) Heart:body mass ratios were precisely maintained in both unaffected and SMA mice, even as SMA mice lost one fifth of their body weight. (**C**) Heart:body length ratios were maintained between genotypes and time points.

maintained, with values comparable between both groups and ages (Fig. 5B). Equivalent ratios of heart to body length were also observed between both groups and time points (Fig. 5C). These data suggest first that heart to body size is precisely maintained in both SMA and heterozygous mice, so the decline in SMA body mass does not appear to result from the developing SMA mouse 'outgrowing' its cardiac size nor from relative cardiac hypertrophy. Second, the hearts of SMA mice appear to be losing mass at the end stages of disease, since their mass ratio is precisely maintained even as the mice lose one-fifth of their body mass.

Heart rate in healthy mice is controlled by a balance of the sympathetic and vagal components of the ANS. Sympathetic nerve activity accelerates the heart rate, whereas the vagal system decelerates it. Arrhythmia characterized by bradycardia and progressive heart block as detected here can result from an autonomic imbalance resulting from decreased sympathetic tone relative to vagal tone. To investigate whether such a decrease in sympathetic innervation may be present, we harvested hearts from PND12 mice and performed whole-mount immunostaining with an antibody to tyrosine hydroxylase (TH), a marker of sympathetic nerves (Fig. 6). We found distinct differences in the TH staining pattern of SMA mice versus controls in both ventral and dorsal views. Ventral views of unaffected hearts contained prominent neurons not observed in SMA hearts (Fig. 6A and B). In dorsal views, we observed that TH-positive neurons from SMA mice seemed to have fewer branches while also appearing thinner and less distinct (Fig. 6C and D), though fine structure was still present upon higher magnification. Quantification of the two most prominent sympathetic neurons visible in the dorsal view of the heart confirmed that there were fewer major neuronal branches detected in SMA hearts (Fig. 6E; $n = 7$ mice per group, $P \leq 0.05$). These results, in conjunction with the types of arrhythmia we observed, suggest that there is a decrease in sympathetic tone present in SMA mice resulting in autonomic imbalance.

Drug treatment improves SMA motor function throughout extended survival

With SMA mouse models becoming a common system for preclinical drug studies, we next sought to explore the utility of ECG as a non-invasive biomarker. Additionally, we wanted to gain insight into the effects that a drug established to display positive-acting effects in SMA mice has on novel cardiac phenotypes we observed, alongside the effects on motor function and survival. For these studies, we chose to use trichostatin A (TSA). TSA, a histone deacetylase inhibitor, has previously been shown to increase SMN transcription and protein both *in vitro* and *in vivo* and to provide benefits to motor function and survival of SMA model mice (21,28). Here, SMA and unaffected heterozygous littermate mice were injected once daily with either TSA at 10 mg/kg or an equivalent volume of vehicle (DMSO) beginning at PND2. ECG was performed on even numbered days by a reader blinded to genotype, drug identity and phenotyping studies, with a sample size of 10 mice per group. Motor function was assayed by measuring the time to right after the placement of each mouse on its back, which was done on each odd numbered day to prevent the elevation of heart rate by a physical activity.

As expected, injection with TSA successfully improved survival, body weight and motor function of SMA mice (Fig. 7). Induction of SMN levels and histone acetylation was also confirmed through molecular analyses (Supplementary Material, Fig. S1). Survival of SMA mice was increased to a median of 22 days when compared with 15.5 days for those injected with vehicle ($P < 0.0005$) (Fig. 7B). Body weights of SMA and unaffected groups were comparable at PND2 and PND4, with vehicle-injected SMA mice weighing 2.5 ± 0.5 g versus unaffected mice weighing 2.7 ± 0.4 g at PND4 (Fig. 7C). After this, SMA mice were lower in weight than unaffected littermates ($P < 0.005$). TSA produced a weight benefit in SMA mice beginning at PND10, at which point vehicle-injected SMA mice began to lose weight, whereas TSA-treated SMA mice continued to gain/maintain weight until approximately PND20. Motor function benefits were observed in SMA mice from PND6 onwards upon TSA treatment (Fig. 7D). Interestingly, TSA improved the motor function of SMA mice through righting time towards levels comparable to unaffected controls through PND21, though many reached death endpoints during this time or shortly after. Maintenance of motor function at late time points was further demonstrated using ambulation and negative geotaxis assays (Supplemental Material, Videos S1–S4). Thus, TSA-treated SMA mice with

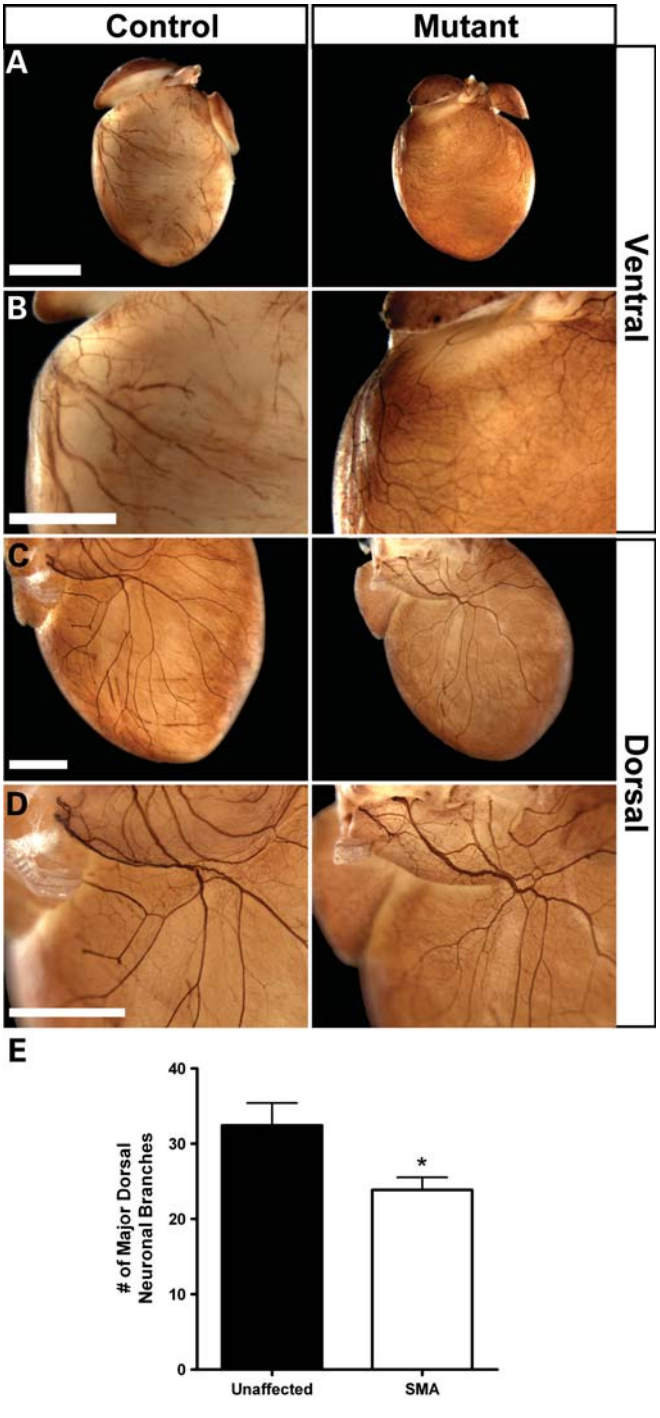

Figure 6. SMA hearts show a decrease in sympathetic staining. Whole-mount immunostaining with an antibody to TH was used to visualize sympathetic innervation. Hearts were harvested from PND12 SMA mice and unaffected littermates. (**A**) Reduced sympathetic patterning was visible in ventral views of representative hearts, further visible by lack of prominent neurons in enlarged views of the right ventricle (**B**). Dorsal views of representative hearts displayed a decrease in neuronal branching (**C**) and neurons that appeared to be thinner with a reduction in staining intensity (**D**). Fine structure was still visible in high magnifications. (**E**) Quantification confirmed a reduction of neuronal branching. Values represent mean ± SEM of total observed branches counted from the two largest neurons present in dorsal views of the heart ($^*P < 0.05$, $n = 7$ hearts per genotype). Scale bars are equivalent to 2000 μm (A) or 1000 μm (B–D).

extended survival were frequently found to die without experiencing a visible decline in motor function.

TSA prolongs heart beat maturation until death of SMA mice

Heart rates of SMA mice were significantly elevated at PND10–14 upon TSA treatment, along with concurrent decreases in PR and QRS interval durations (Fig. 8). These benefits appeared to be maintained until approximately PND20, after which we observed the progression of bradycardia associated with mice reaching death endpoints. In regard to heart rate, we observed no difference between treated and untreated SMA mice before the age of PND10 (Fig. 8A). Before this point, both groups displayed slopes of heart rate growth that were parallel to those of unaffected mice. At PND10 and onward, however, the vehicle group was found to decline significantly, whereas drug-injected mice continued to exhibit a rate of increase comparable to unaffected mice for several more time points. In unaffected littermates, TSA-injected mice showed a trend of lower heart rates; however, this difference was not significant and was present between these groups at PND2, before the first injection.

First-degree heart block was still present in SMA mice upon TSA treatment, though we did not observe the same progression seen in vehicle or untreated SMA mice (Fig. 8B). We found a sharp increase in PR interval duration at PND22, but did not observe highly erratic and/or skipped beats as were detected in untreated SMA mice. Consistent with a lack of breakdown in heart rate regularity, we observed no increase in measures of heart rate variability in TSA-treated SMA mice over that found in unaffected littermates of either treatment group at any time point (Fig. 8C).

Time of ventricular depolarization improved upon drug treatment. Values for QRS interval duration in treated SMA mice were equivalent to those in unaffected littermates from PND10 to PND14 (Fig. 8D). However, at the end stage of life, this was not maintained, as SMA mice showed an increased QRS interval when nearing a death endpoint over unaffected littermates (15.1 ± 5.4 versus 9.38 ± 0.6; $P < 0.05$).

TSA treatment increases the size of SMA hearts

We next investigated the cardiac morphology in SMA mice and our treatment groups at PND12, when clear electrocardiographic differences are present. Observations of heart morphology in vehicle-injected mice were consistent with those in mice that received no injections. Upon dissection, hearts from vehicle-injected SMA mice appeared grossly undersized and flaccid (Fig. 9A). In contrast, TSA-treated SMA mice possessed larger hearts that were closer in size to unaffected mice injected with TSA. In addition, both groups treated with TSA were smaller than unaffected mice injected with vehicle ($P < 0.005$). Hematoxylin and eosin staining of hearts from vehicle-injected SMA mice revealed gross attenuation of walls and dilated cardiomyopathy (Fig. 9B and C). Often, this resulted in hearts that appeared misshapen or 'deflated' and again was consistent with histological observations from SMA mice receiving no injections (data not shown). Upon

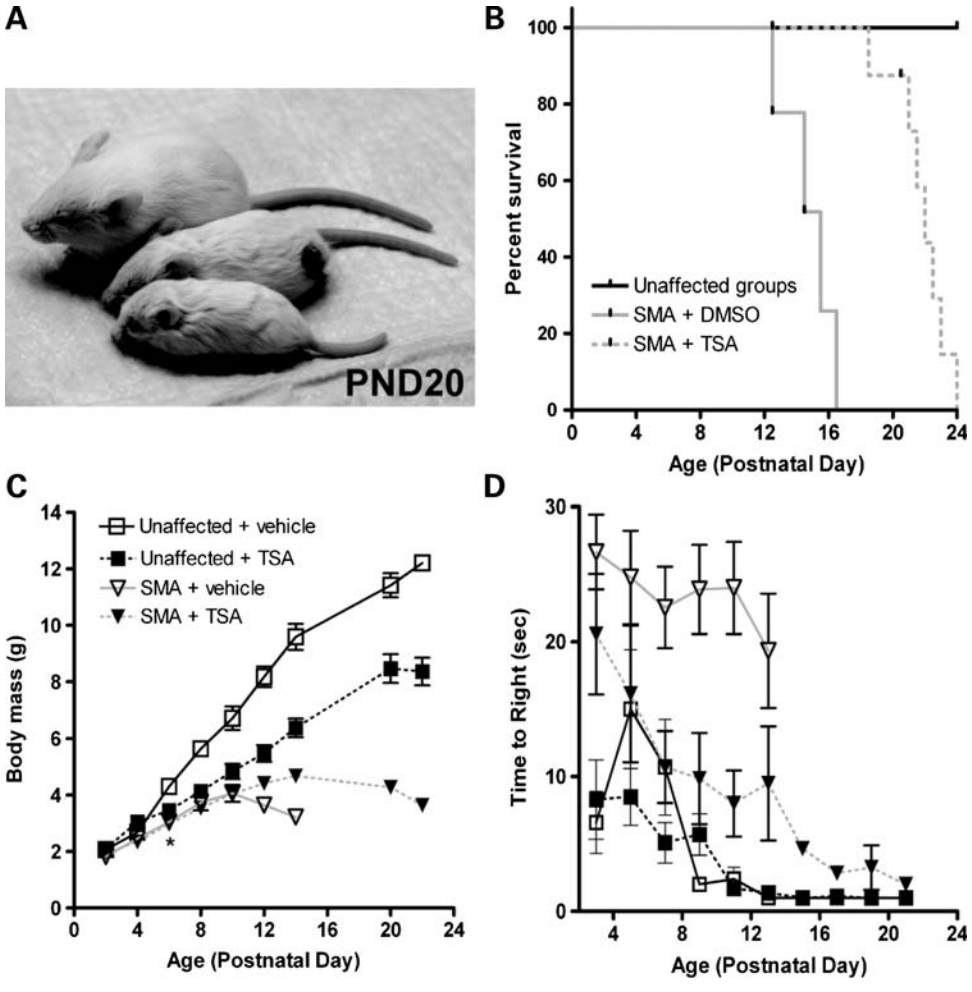

Figure 7. TSA improves motor function throughout extended survival. TSA was administered to SMA mice and unaffected heterozygous littermates at 10 mg/kg by IP injection once daily beginning at PND2. Control groups received an equivalent volume of vehicle (DMSO). (**A**) Mice that are unaffected injected with vehicle (top), unaffected injected with TSA (middle) and SMA treated with TSA (bottom) are pictured. No SMA mice injected with vehicle lived beyond 16 days. (**B**) Kaplan–Meier survival curve of treatment groups. TSA treatment extended SMA survival to a median of 22 days, compared with 15.5 days for vehicle-injected mice (log-rank test, $P < 0.0005$, $n = 10$ mice per group). (**C**) Body mass of mice was comparable between SMA and unaffected littermate groups at PND2 and PND4. Significant reduction in weight of SMA mice compared with unaffected controls was observed beginning on PND6 ($^{*}P < 0.005$, $n = 10$ mice per group). (**D**) Time to right for SMA mice improved to values comparable with unaffected littermates upon TSA treatment. This improvement was maintained as mice reached time points corresponding to death endpoints.

TSA treatment, SMA hearts more closely resembled those of unaffected mice injected with TSA.

Treatment with TSA resulted in hearts that were larger in proportion to body size than in mice injected with vehicle (Fig. 9D). This was true for the heart:body mass ratio of both SMA and unaffected mice ($P < 0.05$, $n \geq 5$ hearts per group). Drug-treated SMA mice also showed an increase in the ratio of the length of their heart to their body ($P < 0.05$) (Fig. 9E). At this time, SMA mice treated with drug were continuing to gain body weight. Thus, SMA mice appear to have hearts that are larger both in weight and in volume when treated with TSA and do not appear to lose cardiac mass at this stage of their life as was found for untreated mice at PND13.

DISCUSSION

Here, we provide the first evidence that cardiac arrhythmias and abnormalities are a feature of SMA model mice. In the clinic, case studies are mounting, which suggest that this may be true in SMA patients as well. We find that SMA mice suffer from congenital bradyarrhythmia and heart block. The end stage of their life is characterized by the progression of these two features to cardiac standstill. Patients in recent studies have shown similar cardiac arrhythmias, autonomic defects and/or cardiomyopathies at what appears to be developing into a higher than chance co-occurrence (Table 1), with severe symptomatic bradycardia being observed in severe forms of SMA and progressive heart block also found in mild or adult onset cases of SMA.

Natural history of SMA ECGs and clinical relevance

ECG studies of SMA mice throughout development reveal severe bradycardia characterized by progressive heart block and impaired ventricular conduction. At early time points, heart rate parameters are elongated but appear to mature at

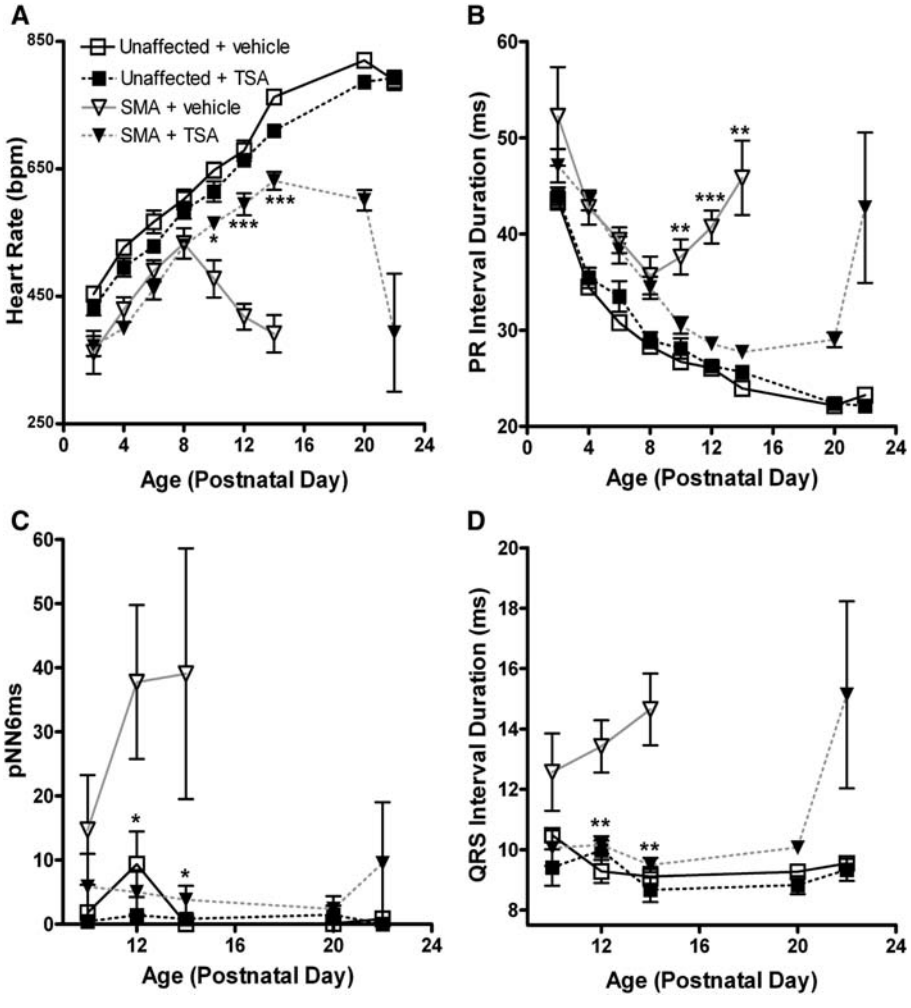

Figure 8. ECG of TSA treatment groups. Extended maturation of ECG waveforms was observed in SMA mice treated with TSA. ECGs were obtained every 2 days from PND2 to PND14, with all animals conscious and unrestrained. (**A**) Heart rate, (**B**) PR interval, (**C**) pNN6ms and (**D**) QRS interval all expressed as mean ± SEM ($^{*}P < 0.01$, $^{**}P < 0.001$, $^{***}P < 1E^{-5}$, $n = 10$ mice per data point).

rates that closely parallel those of unaffected littermates, despite the onset of large differences in both the rate of growth displayed by mice (setting in around PND3 and PND4) and motor function. At the end stage of disease, approximately 4–6 days preceding death, we see a sharp progression of ECG deficits as mice develop severe symptomatic bradycardia and higher degree heart block, ultimately leading to cardiac standstill. Although thorough ECG natural histories of SMA patients are currently lacking in the literature, several groups have noted precisely these two features of severe symptomatic bradycardia and progressive heart block in both random pools and isolated cases of SMA patients (5–8).

We find evidence of both myocardial and ANS deficits present in SMA mice. Cases of both autonomic and myocardial defects are also found in clinical studies (9–11,16). Instances of each are also found in other neuromuscular and motor neuron diseases (29–37). Respiratory distress, typically the ultimate cause of death in SMA and other neuromuscular diseases, can further exacerbate arrhythmia and myocardial defects by putting the body into states of oxidative and/or metabolic stress. At the end stages of the disease in SMA mice, we do see an exacerbation of ECG deficits consistent with such an event. Therefore, the ECG natural history we provide may be accurately describing the SMA death process of these mice.

Impaired cardiac function present by PND2

Quantitative consistency in gaging the onset of disease phenotypes in fragile groups of mice such as those studied here can be difficult. This can be further complicated by subjective calls in applying motor scales and by inter-rater variability. Previous investigations describe the onset of neuromuscular symptoms in the *SMNΔ7* mouse model as becoming apparent around PND5 (19–20,28,38–40). Others have predicted identifiable phenotypic differences at earlier time points when using large numbers (greater than 60) of mice (41). Here we readily detect impaired cardiac function using a system that is automated, non-invasive and requires no restraint or anesthesia. We find clear differences present in relatively small groups

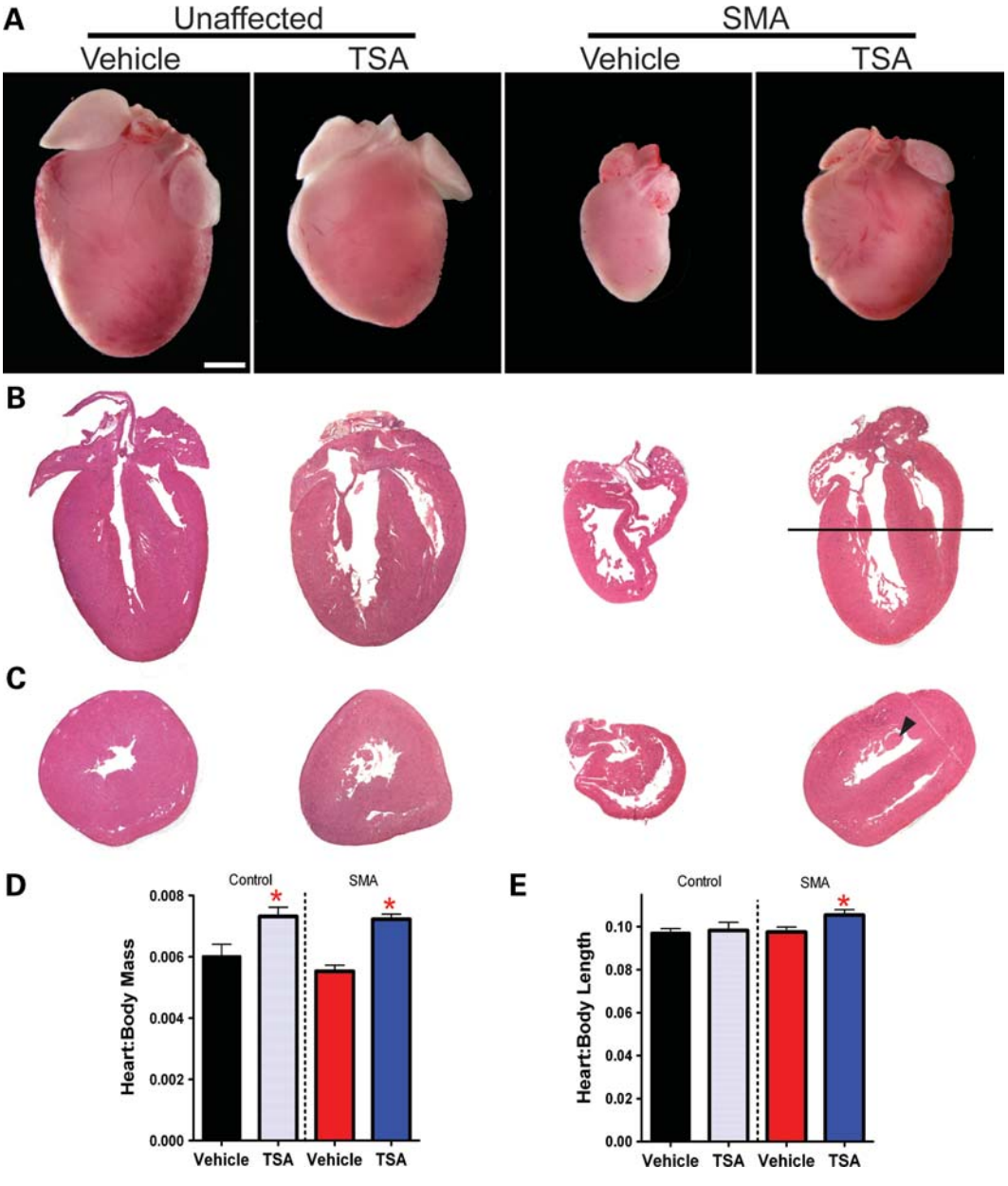

Figure 9. Cardiac morphology of SMA treatment group hearts. Hearts harvested from SMA mice injected with vehicle were smaller than those of unaffected littermates and typically appeared flaccid or unable to hold their shape. TSA treatment corresponded with an increase in heart:body ratio and an increase in the absolute mass of SMA hearts. (**A**) Images of hearts representative for each treatment group, from at least five hearts per group. (**B** and **C**) Hematoxylin and eosin staining of representative heart sections revealed cardiomyopathy in vehicle SMA mice characterized by gross attenuation of walls and dilation of ventricles. Sections in (B) are cut in a longitudinal orientation to display the four chambers of the heart. A black line represents the level at which additional hearts were cut in a cross-sectional direction for images in (C), where the papillary muscle used as a point of reference is denoted in the TSA-treated SMA heart by a black arrowhead. (**D**) Heart:body mass ratios were increased in TSA-treated groups of mice. (**E**) Heart:body length ratios were increased in TSA-treated SMA mice only ($^{*}P < 0.05$, $n = 5–6$ hearts per treatment group).

of mice as early as PND2, with heart rates that are reduced by greater than 20% of littermate controls and PR intervals that are elevated by ~15%. At this point, mice are weight-matched and do not display consistent, quantifiable motor function deficits.

Functional deficit of SMA hearts is further validated by echocardiography at PND6, at which point we observe a decrease in hemodynamics at the pulmonary valve of the right ventricle. Such a decrease represents a functional reduction in the hearts' ability to move deoxygenated blood to the lungs. In an organism that is modeling a human disease where respiratory distress is a primary health concern, this could represent a significant health deficit for SMA mice. Together, our data present the first evidence of impaired cardiac function in SMA mice and establish new, quantitative phenotypes that are readily detectable as early as PND2.

Table 1. Clinical co-occurrence of arrhythmia, cardiomyopathy and ANS defects with SMA

Reference	SMA type	Inclusion criteria and sample size	Type of abnormality	Finding	# Observed (% of total)
Bach (5)	I	All 63 patients attending 1 clinic	Arrhythmia	LOC w/**severe bradycardia**, four died from progression to standstill	15 (24%)
	II	Observed, not reported	Arrhythmia	LOC w/ **severe bradycardia**	
Roos *et al*. (7)	Adult onset	2 related individuals	Arrhyhtmia	**AV block**	Both
Elkohen *et al*. (6)	III	8 random cases	Cardiomyopathy	**Fatal dilated cardiomyopathy, reduced SF detected via echo**	1 (13%)
			Arrhythmia	**Symptomatic conduction disease, progressive AV block**	1 (13%)
Tanaka *et al*. (8)	III	1 isolated case	Arrhythmia	**Complete AV block**, atrial flutter	
			Cardiomyopathy	Fibrosis of right ventricle	
Schoneborn *et al*. (18)	I (1 copy)	4 random cases	CHD	ASD, VSD, PDA, **dilated ventricle**	3 (75%)
			Arryhthmia	Fetal, tachycardia, **bradycardia**	
	I (2 copies)	56 random cases	Minor cardio	PFO, PDA, VSD	6 (11%)
Araujo Ade *et al*. (10)	I	2 unrelated cases	Vascular	Poor perfusion, **digital necrosis**	2 (100%)
			ANS	Hyperhidrosis, absent reflexes	1 (50%)
			Cardiomyopathy	ASD and asymmetric VH	1 (50%)
Arai *et al*. (9)	I and II	9 random cases	ANS	Hyperhydrosis, decreased SSRs and vasodilation response	7 (77%)
			Arrhythmia	Resting tachycardia	7 (77%)
			Arrhythmia	Abnormal **RR variation**	3 (33%)
Hachiya *et al*. (11)	I	2 cases with extended survival	Arrhythmia	Abnormal **RR variation**	2 (67%)
			ANS	Affected vasodilation response	2 (67%)
			Arrhythmia	Paroxysmal tachycardia	
Tanaka *et al*. (16)	III	1 isolated case	Cardiomyopathy	EM:loss of myosin filaments, Z-band defects, leptomeric fibrils	

CHD, congenital heart disease; ASD, atrial septal defect; SF, shortening fraction; VSD, ventricular septal defect; PDA, patent ductus arteriosus; PFO, patent foramen ovale; VH, ventricular hypertrophy; SSRs, sympathetic skin response to sound; EM, electron microscopy. Conditions also observed in SMA model mice are denoted in bold.

ECG of drug treated mice

Maturation of neonatal heart rate in healthy mice is linear, with a rate of approximately 25 b.p.m. each day (22). Untreated SMA mice deviate from this maturation pattern beginning at PND10, with a decreased rate of growth and/or crash in heart rate. Treatment of SMA mice with TSA corrected this, resulting in SMA mice with extended periods of normal ECG maturation rates. Mass and body temperature do not appear to cause the reduction in heart rate in SMA mice, because at periods when the slope of SMA heart rate maturation is comparable to healthy mice, these mouse groups have very different growth rates and are known to possess opposite trends of body temperature (39). Specific time points when groups here have comparable body mass but very different ECGs (PND2, 4 and 10) support this. Thus, these data show that discrepancies in ECG are not simply a consequence of differences in size, body temperature or growth rate of SMA mice. It instead suggests that, since cardiac function is impaired at a very early age, a decrease in the ability of the SMA heart to supply blood to rapidly developing neonates may actually cause or contribute to the stunted growth and body temperature development of SMA mice.

Untreated SMA mice show a decrease in their LOC in conjunction with the progression of bradyarrhythmia, heart block, weight loss and motor function decline beginning around PND10. TSA-treated SMA mice with extended survival eventually died without exhibiting a clear loss of motor function, yet we were able to detect a progression of bradyarrhythmia and weight loss. This suggests that progression of arrhythmia may be both predictive of a death event and separate from that of neuromuscular function in SMA mice. Together, these findings establish non-invasive ECG as a sensitive and quantitative index of SMA mouse health.

Conclusions and working model

Based on the compilation of our data and SMA patient case reports, we propose that low levels of SMN, besides contributing to motor neuron loss, also result in a primary autonomic imbalance. In the *SMNΔ7* mouse model of SMA, this manifests as a decrease in sympathetic innervation. Such an imbalance would be characterized by a relative increase in vagal tone, which is consistent with the manifestation of bradycardia and progressive heart block observed here. Resulting functional deficits at critical developmental periods could prevent proper myocardial development and/or induce secondary myocardial defects. Cardiac insufficiency could also slow the growth rate of neonate mice and be compounded as mice, unable to maintain rapid development, enter states of cardiorespiratory/oxidative/metabolic distress. Such events are observed in SMA mice around the ages of PND4 through a reduction in growth rate and of PND10 when there is a decrease in LOC, onset of weight loss and exacerbation of arrhythmias. During these ages, maturation of autonomic neurotransmission and control of heart rate is still occurring

in small mammals (25,42–43). From a therapeutics standpoint, it follows that therapeutic intervention may be sufficient to enable mice to live through a critical period in cardiac development; however, SMA mice may still succumb to autonomic and/or motor neuron defects at later stages, visible by increased sudden death or downstream decline in motor/respiratory function.

With the importance that mouse models now hold in SMA preclinical studies, it will be of significant value to investigate these issues. The more we understand their full extent and rescue in mouse models, the better we will be able to translate therapeutics into our clinics. Towards that end, transgenic strategies that induce SMN specifically in autonomic or myocardial tissues could elucidate their ability to benefit murine SMA. Further developmental profiling of these defects will be useful to resolve the timing of their onset, particularly embryonically and in comparison with SMA symptoms and motor neuron defects. Since questions of primary versus secondary cardiac phenotypes can be difficult to resolve in mice with a severe phenotype and early/neonatal lethality, less severe SMA models should also be characterized for cardiac phenotypes and could provide systems for further insight. For example, longer-lived models would be amenable to telemetry ECG to detect transient arrhythmia events and would provide clearer systems of study to test for other autonomic defects and ANS targeting drug effects.

The clear functional cardiac deficits in SMA mice, together with mounting case studies and instances in comparable diseases, underscore several important clinical points of interest for SMA research moving forward as well. First, the effects of SMN reduction on proper cardiac/ANS development should be investigated. Further, there is a need for larger-scale, randomized clinical studies to determine the true co-occurrence of arrhythmia and cardiomyopathy. Lastly, as we develop clinical therapeutics that extend patient survival, it will be important to monitor SMA patients for the unmasking of previously hidden cardiac pathologies.

MATERIALS AND METHODS

Animal maintenance and drug treatment

SMA model mice (strain #005025) were purchased from The Jackson Laboratories. Production and initial characterization of this SMA mouse model has been previously reported (19). All animals were maintained in a controlled animal facility at 20°C and 50% humidity, with a photoperiod of 12 h light/12 h dark where they were monitored daily for health as described previously (20). Mice were fed *ad libitum* for water and food on a Harlan 6% crude fat diet. All maintenance and procedures were approved and performed in accordance with the Children's Memorial Research Center's Institutional Animal Care and Use Committee (IACUC) and Jackson Laboratories regulations.

An SMA transgenic colony was maintained by mating $SMN2^{+/+}$;$SMN\Delta7^{+/+}$;$Smn^{+/-}$ breeding mice. Mice were genotyped for the *Smn* knockout allele as described previously (20). Mice were monitored daily for weight and survival. Righting time was measured every other day as a measure of motor function, with times representing the lower time of two attempts and failure to right given the maximum allowed time of 30 s. When mice were considered to have met functional death endpoints (20% loss of body weight, inability to right within 30 s and/or obvious state of distress), mice were euthanized with CO_2 followed by cervical dislocation as a secondary measure. In this and previous work, we have found the earliest mortality of uninjected SMA mice to be PND8 (20). Any injected mice dying before this age were assumed to have died from other causes (injection injury, cannibalism, malnutrition etc.) and any data from them excluded from the analysis. For drug treatments, TSA (BIOMOL) was dissolved in DMSO to a stock concentration of 8 mg/ml active solution and stored at −20°C. Preceeding injection into selected animals, stock TSA was thawed and diluted 1:1 with saline. SMA and unaffected heterozygous mice were administered 10 mg/kg TSA or an equivalent volume of DMSO vehicle diluted 1:1 with saline by intraperitoneal injection once daily from PND2 to PND14, with surviving SMA mice continuing to receive injections until PND20 or until they met a functional death endpoint.

Electrocardiogram

ECGs were recorded non-invasively in conscious mice using the ECGenie system (Mouse Specifics). Recordings were performed every 2 days from PND2 through PND14. Neonate mice were placed inside a temperature-controlled heated cup positioned on the ECG platform set to maintain a temperature of 30°C. Body temperatures were measured on a subset of mice using an infrared thermometer to verify consistency before and after taking ECG readings. For treated SMA mice surviving to weanling time points, readings were obtained on PND20 and PND22. Briefly, mice were placed on a small platform instrumented with ECG recording electrodes and allowed to acclimate for ∼10 min. After the acclimation period, ECG signals were recorded for ∼5 s while the mice passively established contact between the underside of their paws and the electrodes. Data acquisition was carried out using the program LabChart 6 (ADInstruments). Analysis of individual ECGs was then performed using the e-MOUSE physiologic waveform analysis portal (23). Heart rate variability was assayed through the pNN6ms time domain statistic, which represents the percentage of adjacent RR intervals that differ by a length of time exceeding the experimental threshold (6 ms). Data presented represent mean ± SD unless otherwise noted. Statistical comparison between groups was performed by Student's *t*-test. Differences were considered significant when $P \leq 0.05$.

Cardiac histology and immunostaining

At selected time points, animals were sacrificed and measured for body length before harvesting the tissues for further analyses. Liver, lungs and hearts were removed and weighed. For morphology studies, hearts were fixed in Bouin's fixative, then measured for length and stored in 50% ethanol. Hematoxylin and eosin staining was performed on 5 μm sections of Paraffin-embedded tissue. For innervation studies, hearts were fixed in SafeFix (Fisher) fixative. An antibody for TH (Chemicon) was used at the dilution of 1:100 in 5% BSA block, followed

by GAR at 1:500 (Bio-Rad). Nerves were then stained with DAB (Sigma), cleared by immersion in 20% glycerol and 0.25% KOH and imaged with a Leica M125 dissecting light microscope.

Echocardiography

Echocardiogram analyses were performed at The Jackson Laboratories. Briefly, mice were anesthetized with isofluorane (1–1.5% at 0.6 l/min). Echocardiograms were then carried out using a Vevo 770 high-frequency ultrasound system (VisualSonics) with a RMV 707B scan-head in the parasternal outflow view. From these images, the peak velocity and peak gradient were measured at the pulmonary valve.

SUPPLEMENTARY MATERIAL

Supplementary Material is available at *HMG* online.

ACKNOWLEDGEMENT

We would like to thank Dr Thomas Hampton and Ajit Kale for technical assistance in analyzing waveforms.

Conflict of Interest statement. None declared.

FUNDING

This work was supported by the National Institutes of Health (1RO1NS060926-01, 1R21HD058311-01A1, 3R01NS060926-02S3), the Families of Spinal Muscular Atrophy (DiD0809) and the Medical Research Junior Board Foundation at Children's Memorial Hospital. C.H. is supported by Northwestern University's Presidential Fellowship.

REFERENCES

1. Crawford, T.O. and Pardo, C.A. (1996) The neurobiology of childhood spinal muscular atrophy. *Neurobiol. Dis.*, **3**, 97–110.
2. Lefebvre, S., Burglen, L., Reboullet, S., Clermont, O., Burlet, P., Viollet, L., Benichou, B., Cruaud, C., Millasseau, P., Zeviani, M. *et al.* (1995) Identification and characterization of a spinal muscular atrophy-determining gene. *Cell*, **80**, 155–165.
3. Rochette, C.F., Gilbert, N. and Simard, L.R. (2001) SMN gene duplication and the emergence of the *SMN2* gene occurred in distinct hominids: SMN2 is unique to *Homo sapiens*. *Hum. Genet.*, **108**, 255–266.
4. Wirth, B. (2000) An update of the mutation spectrum of the survival motor neuron gene (*SMN1*) in autosomal recessive spinal muscular atrophy (SMA). *Hum. Mutat.*, **15**, 228–237.
5. Bach, J.R. (2007) Medical considerations of long-term survival of Werdnig–Hoffmann disease. *Am. J. Phys. Med. Rehabil.*, **86**, 349–355.
6. Elkohen, M., Vaksmann, G., Elkohen, M.R., Francart, C., Foucher, C. and Rey, C. (1996) Cardiac involvement in Kugelberg–Welander disease. A prospective study of 8 cases. *Arch. Mal. Coeur. Vaiss.*, **89**, 611–617.
7. Roos, M., Sarkozy, A., Chierchia, G.B., De Wilde, P., Schmedding, E. and Brugada, P. (2009) Malignant ventricular arrhythmia in a case of adult onset of spinal muscular atrophy (Kugelberg–Welander disease). *J. Cardiovasc. Electrophysiol.*, **20**, 342–344.
8. Tanaka, H., Uemura, N., Toyama, Y., Kudo, A. and Ohkatsu, Y. (1976) Cardiac involvement in the Kugelbert–Welander syndrome. *Am. J. Cardiol.*, **38**, 528–532.
9. Arai, H., Tanabe, Y., Hachiya, Y., Otsuka, E., Kumada, S., Furushima, W., Kohyama, J., Yamashita, S., Takanashi, J. and Kohno, Y. (2005) Finger cold-induced vasodilatation, sympathetic skin response, and R–R interval variation in patients with progressive spinal muscular atrophy. *J. Child Neurol.*, **20**, 871–875.
10. Araujo Ade, Q., Araujo, M. and Swoboda, K.J. (2009) Vascular perfusion abnormalities in infants with spinal muscular atrophy. *J. Pediatr.*, **155**, 292–294.
11. Hachiya, Y., Arai, H., Hayashi, M., Kumada, S., Furushima, W., Ohtsuka, E., Ito, Y., Uchiyama, A. and Kurata, K. (2005) Autonomic dysfunction in cases of spinal muscular atrophy type 1 with long survival. *Brain Dev.*, **27**, 574–578.
12. El-Matary, W., Kotagiri, S., Cameron, D. and Peart, I. (2004) Spinal muscle atrophy type 1 (Werdnig–Hoffman disease) with complex cardiac malformation. *Eur. J. Pediatr.*, **163**, 331–332.
13. Menke, L.A., Poll-The, B.T., Clur, S.A., Bilardo, C.M., van der Wal, A.C., Lemmink, H.H. and Cobben, J.M. (2008) Congenital heart defects in spinal muscular atrophy type I: a clinical report of two siblings and a review of the literature. *Am. J. Med. Genet. A*, **146A**, 740–744.
14. Moller, P., Moe, N., Saugstad, O.D., Skullerud, K., Velken, M., Berg, K., Nitter-Hauge, S. and Borresen, A.L. (1990) Spinal muscular atrophy type I combined with atrial septal defect in three sibs. *Clin. Genet.*, **38**, 81–83.
15. Mulleners, W.M., van Ravenswaay, C.M., Gabreels, F.J., Hamel, B.C., van Oort, A. and Sengers, R.C. (1996) Spinal muscular atrophy combined with congenital heart disease: a report of two cases. *Neuropediatrics*, **27**, 333–334.
16. Tanaka, H., Nishi, S., Nuruki, K. and Tanaka, N. (1977) Myocardial ultrastructural changes in Kugelberg–Welander syndrome. *Br. Heart J.*, **39**, 1390–1393.
17. Vaidla, E., Talvik, I., Kulla, A., Sibul, H., Maasalu, K., Metsvaht, T., Piirsoo, A. and Talvik, T. (2007) Neonatal spinal muscular atrophy type 1 with bone fractures and heart defect. *J Child Neurol.*, **22**, 67–70.
18. Rudnik-Schoneborn, S., Heller, R., Berg, C., Betzler, C., Grimm, T., Eggermann, T., Eggermann, K., Wirth, R., Wirth, B. and Zerres, K. (2008) Congenital heart disease is a feature of severe infantile spinal muscular atrophy. *J. Med. Genet.*, **45**, 635–638.
19. Le, T.T., Pham, L.T., Butchbach, M.E., Zhang, H.L., Monani, U.R., Coovert, D.D., Gavrilina, T.O., Xing, L., Bassell, G.J. and Burghes, A.H. (2005) SMNDelta7, the major product of the centromeric survival motor neuron (*SMN2*) gene, extends survival in mice with spinal muscular atrophy and associates with full-length SMN. *Hum. Mol. Genet.*, **14**, 845–857.
20. Heier, C.R. and DiDonato, C.J. (2009) Translational readthrough by the aminoglycoside geneticin (G418) modulates SMN stability *in vitro* and improves motor function in SMA mice *in vivo*. *Hum. Mol. Genet.*, **18**, 1310–1322.
21. Narver, H.L., Kong, L., Burnett, B.G., Choe, D.W., Bosch-Marce, M., Taye, A.A., Eckhaus, M.A. and Sumner, C.J. (2008) Sustained improvement of spinal muscular atrophy mice treated with trichostatin A plus nutrition. *Ann. Neurol.*, **64**, 465–470.
22. Heier, C.R., Hampton, T.G. and DiDonato, C.J. (2010) Development of electrocardiogram intervals during growth of FVB/N neonate mice. In press.
23. Chu, V., Otero, J.M., Lopez, O., Morgan, J.P., Amende, I. and Hampton, T.G. (2001) Method for non-invasively recording electrocardiograms in conscious mice. *BMC Physiol.*, **1**, 6.
24. Harper, R.M., Leake, B., Hodgman, J.E. and Hoppenbrouwers, T. (1982) Developmental patterns of heart rate and heart rate variability during sleep and waking in normal infants and infants at risk for the sudden infant death syndrome. *Sleep*, **5**, 28–38.
25. Hofer, M.A. and Reiser, M.F. (1969) The development of cardiac rate regulation in preweanling rats. *Psychosom. Med.*, **31**, 372–388.
26. Schechtman, V.L., Harper, R.M., Kluge, K.A., Wilson, A.J., Hoffman, H.J. and Southall, D.P. (1988) Cardiac and respiratory patterns in normal infants and victims of the sudden infant death syndrome. *Sleep*, **11**, 413–424.
27. Siimes, A.S., Valimaki, I.A., Sarajas, H.S., Sakone, K. and Oja, R.T. (1984) Heart rate variation in relation to age and sleep state in neonatal lambs. *Acta. Physiol. Scand. Suppl.*, **537**, 7–15.
28. Avila, A.M., Burnett, B.G., Taye, A.A., Gabanella, F., Knight, M.A., Hartenstein, P., Cizman, Z., Di Prospero, N.A., Pellizzoni, L., Fischbeck, K.H. *et al.* (2007) Trichostatin A increases SMN expression and survival in a mouse model of spinal muscular atrophy. *J. Clin. Invest.*, **117**, 659–671.
29. Maddatu, T.P., Garvey, S.M., Schroeder, D.G., Hampton, T.G. and Cox, G.A. (2004) Transgenic rescue of neurogenic atrophy in the nmd mouse reveals a role for Ighmbp2 in dilated cardiomyopathy. *Hum. Mol. Genet.*, **13**, 1105–1115.

30. Maddatu, T.P., Garvey, S.M., Schroeder, D.G., Zhang, W., Kim, S.Y., Nicholson, A.I., Davis, C.J. and Cox, G.A. (2005) Dilated cardiomyopathy in the nmd mouse: transgenic rescue and QTLs that improve cardiac function and survival. *Hum. Mol. Genet.*, **14**, 3179–3189.
31. Rudnik-Schoneborn, S., Stolz, P., Varon, R., Grohmann, K., Schachtele, M., Ketelsen, U.P., Stavrou, D., Kurz, H., Hubner, C. and Zerres, K. (2004) Long-term observations of patients with infantile spinal muscular atrophy with respiratory distress type 1 (SMARD1). *Neuropediatrics*, **35**, 174–182.
32. Asai, H., Hirano, M., Udaka, F., Shimada, K., Oda, M., Kubori, T., Nishinaka, K., Tsujimura, T., Izumi, Y., Konishi, N. *et al.* (2007) Sympathetic disturbances increase risk of sudden cardiac arrest in sporadic ALS. *J. Neurol. Sci.*, **254**, 78–83.
33. Beck, M., Giess, R., Magnus, T., Puls, I., Reiners, K., Toyka, K.V. and Naumann, M. (2002) Progressive sudomotor dysfunction in amyotrophic lateral sclerosis. *J. Neurol. Neurosurg. Psychiatry*, **73**, 68–70.
34. Murata, Y., Harada, T., Ishizaki, F., Izumi, Y. and Nakamura, S. (1997) An abnormal relationship between blood pressure and pulse rate in amyotrophic lateral sclerosis. *Acta. Neurol. Scand.*, **96**, 118–122.
35. Buob, A., Winter, H., Kindermann, M., Becker, G., Moller, J.C., Oertel, W.H. and Bohm, M. (2010) Parasympathetic but not sympathetic cardiac dysfunction at early stages of Parkinson's disease. *Clin. Res. Cardiol.*, **99**, doi:10.1007/s00392-010-0170-6 .
36. Foster, P.S., Drago, V., Harrison, D.W., Skidmore, F., Crucian, G.P. and Heilman, K.M. (2010) Influence of left versus right hemibody onset Parkinson's disease on cardiovascular control. *Laterality*, **15**, 1–10.
37. Tijero, B., Gomez-Esteban, J.C., Llorens, V., Lezcano, E., Gonzalez-Fernandez, M.C., de Pancorbo, M.M., Ruiz-Martinez, J., Cembellin, J.C. and Zarranz, J.J. (2010) Cardiac sympathetic denervation precedes nigrostriatal loss in the E46K mutation of the alpha-synuclein gene (SNCA). *Clin. Auton. Res.*, **20**, 267–269.
38. Baumer, D., Lee, S., Nicholson, G., Davies, J.L., Parkinson, N.J., Murray, L.M., Gillingwater, T.H., Ansorge, O., Davies, K.E. and Talbot, K. (2009) Alternative splicing events are a late feature of pathology in a mouse model of spinal muscular atrophy. *PLoS Genet.*, **5**, e1000773.
39. El-Khodor, B.F., Edgar, N., Chen, A., Winberg, M.L., Joyce, C., Brunner, D., Suarez-Farinas, M. and Heyes, M.P. (2008) Identification of a battery of tests for drug candidate evaluation in the SMNDelta7 neonate model of spinal muscular atrophy. *Exp. Neurol.*, **212**, 29–43.
40. Riessland, M., Ackermann, B., Forster, A., Jakubik, M., Hauke, J., Garbes, L., Fritzsche, I., Mende, Y., Blumcke, I., Hahnen, E. *et al.* (2010) SAHA ameliorates the SMA phenotype in two mouse models for spinal muscular atrophy. *Hum. Mol. Genet.*, **19**, 1492–1506.
41. Butchbach, M.E., Edwards, J.D. and Burghes, A.H. (2007) Abnormal motor phenotype in the SMNDelta7 mouse model of spinal muscular atrophy. *Neurobiol. Dis.*, **27**, 207–219.
42. Adolph, E.F. (1971) Ontogeny of heart-rate controls in hamster, rat, and guinea pig. *Am. J. Physiol.*, **220**, 1896–1902.
43. Navaratnam, V. (1965) The ontogenesis of cholinesterase activity within the heart and cardiac ganglia in man, rat, rabbit and guinea-pig. *J. Anat.*, **99**, 459–467.